

Measurement of Landslide Displacement and Orientation using Strain Gauges Based on Amorphous Magnetic Microwires

Daniel Petrisor, Cristian Fosalau, Cristian Zet, Catalin Damian

“Gheorghe Asachi” Technical University of Iasi
D.Mangeon 23, Iasi, Romania, phone: +40232278680, fax: +40232237627
e-mail: dpetrisor@ee.tuiasi.ro

Abstract- In this paper, we present the performance of a landslide transducer based on magnetic strain gauges and the interpretation of experimental results. Analysis of landslide data indicates that the land displacements measured with our transducer are correlated to the movements measured at the ground surface. Evaluating the landslide data, we have established a relationship between the system readings and the landslide movement. Measurements regarding landslide displacement and orientation were done using strain gauges based on amorphous magnetic microwires (MAW). In order to evaluate a larger area, our system uses a grid of measurement points containing multiple measurement nodes. Each measurement node acquires displacement and orientation information reporting the data through RS485 to the central unit coordinator. Measurement information from central unit coordinators across the grid is transmitted wirelessly to a server for storage and alerting actions.

Keywords: landslide displacement, strain sensor, amorphous magnetic microwires

I. Introduction

Landslide is a phenomenon in which the mass of the surface earth layers slowly displace, moving approximately 0.01mm to 10mm per day. The current technology used for monitoring landslide phenomenon uses expansion gauge, inclinometer and GPS systems [1]. Because usually landslides cover wide surface areas, monitoring the whole landslide area poses constraints regarding equipment and data transmissions. Due to rainfall events, landslide reactivation or acceleration may occur in a short period. For this, the necessity of a system capable to measure in real time a wide range of parameters and to alert the decision factors may arise. In this case, observations made after the event may not contain relevant information referring to the triggering conditions of the landslide displacement. A continuous recording of different environmental parameters such as rainfall, pore water pressures or landslide displacements have become sources of data used to analyze the stability of the slope for better understanding the dynamics of the landslide [2]. Existing landslide monitoring equipment and systems are based on: radar satellite interferometry [3], laser scanning [4], high resolution imaging via satellites [5]. The main disadvantages of these systems are related to high cost, low resolution and discontinuity in the data acquisition. Local sensor-based measurement systems use: GPS - Global Positioning System [6], optical fiber configurations [7], typologies of tilt sensors, acceleration, pressure transducers, etc.. Most of these systems are still using physical connections (cables) between sensors, which is their main disadvantage [8]. The aim of the paper is to present the performance of a landslide displacement and orientation measurement system. Our system measures the displacement using transducers based on strain gauges (SG) mounted on multiple measurement points along a rod placed within a borehole. Grid measurement points placed across the landslide area of interest compose the monitoring system used to measure ground displacements. The measurement point has a central unit coordinator responsible for communicating via RS485 with the measurement nodes placed on the pole. A microcontroller that evaluates the displacement via the measurement bridge composed of four strain gauges manages an intelligent measurement node. Nodes transfer landslide displacement data to the unit coordinator that transmits data packages via a wireless link to a central server. Real time measurement data stored on server are used to survey landslide parameters and create distress alerts.

II. Description of the landslide displacement and orientation measurement system

The proposed system uses a grid of measurement points, as described in Figure 1. Measurement points are managed by a unit coordinator and use multiple measurement nodes composed of a microcontroller and a measurement bridge. The structure of a measurement node is presented in Figure 2(a), while the component connections are shown in Figure 2(b). The strain gauges compose the measurement bridge that is used to measure landslide displacement and orientation. We have used strain gauges having as sensitive element an MAW of 20 mm in the as-cast form of 101 μm diameter, with composition $(\text{Co}_{0,94}\text{Fe}_{0,06})_{72,5}\text{Si}_{12,5}\text{B}_{15}$ [9]. The amorphous magnetic micro wires are bonded on pads and stiffened with cyanoacrylate glue on a polyamide substrate to create the strain gauge. The strain gauges that form a measurement node are bonded onto the surface of the rod whose deformation is to be measured. A measurement point consists of multiple nodes disposed along

the rod mounted in a borehole used to monitor the landslide. In our experiments, the bridge was supplied with a 5mA ac current of 1MHz frequency provided by a microcontroller DAC. This current assures the maximum operating range of the gauge of ± 200 ppm. The characteristic impedance of the gauge in relaxed state has a value Z_0 of 21Ω . The deformations of this transducer, caused by the landslide displacement, were measured along the rod by measurement nodes. A landslide displacement causes variations of the strain gauges impedances by giant magnetoimpedance effect, unbalancing the measurement bridge [10]. These impedance variations are sensed by measuring the variation of potentials in (a) and (b) points of the bridge in Figure 2. Figure 3 presents the variation of potentials in (a) and (b) caused by changes of impedances of strain gauges submitted to deformations caused by landslide displacements. Potentials shown in Figure 3 have been measured by simulating a landslide displacement oriented along the direction given by strain gauges (1) and (2). In this case, impedance variation causing the bridge unbalancing is produced mainly by these devices. The relative variation of impedance, β , has been computed as $\beta = \Delta Z / Z_0 \cdot 100 [\%]$, where Z_0 is the wire impedance without any stress applied.

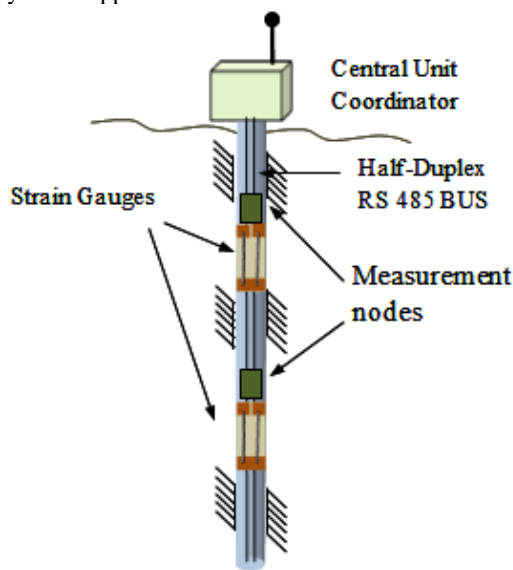


Figure 1. Measurement point structure a) central unit coordinator, b) strain gauges, c) measurement nodes, d) RS485communication BUS

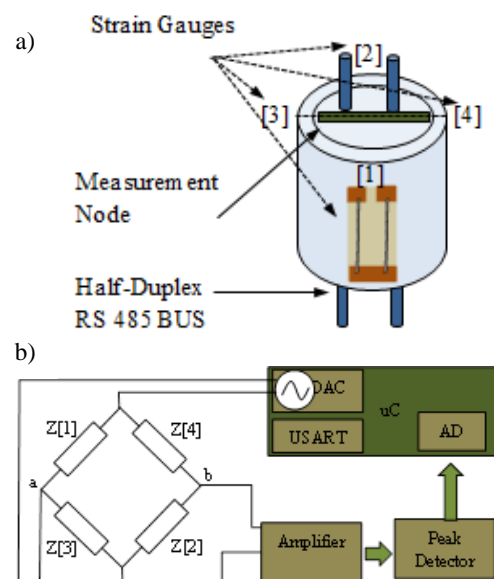


Figure 2. Measurement node components and structure a) measurement node components, b) measurement node connections

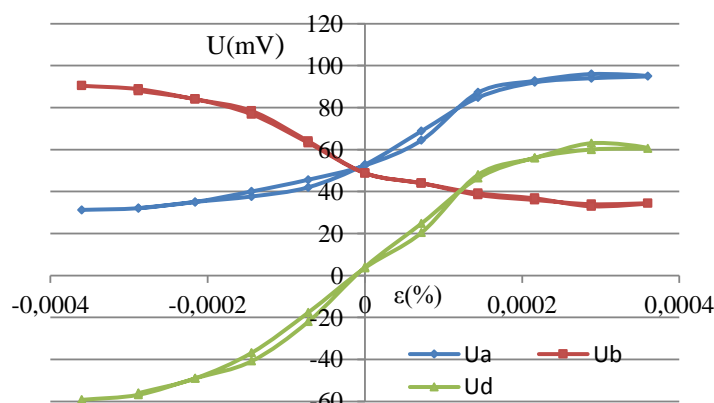


Figure 3. Voltage potentials measured for different deformations of the sensing pole. U_a, U_b potentials correspondent to (a) and (b) points of the measurement bridge, U_d is the potential difference between U_a and U_b

III. Mathematical model for computing landslide displacement and orientation

The orientation and displacement components of the landslide were computed using a complex mathematical model that integrates the impedance variations of all strain gauges composing the bridge. The computational model used to determine the orientation and displacement takes in to consideration the measured potentials U_a , U_b and also physical dimensions of the measurement point structure, like height H and diameter t . Strain gauge

dimensions are included into the computation by means of initial length l_0 , and the length after deformation l_x . The final goal of our complex mathematical model is to compute in the Total Landslide Displacement and Orientation (TLSDO). TLSDO is calculated relatively to the N cardinal direction and is defined in polar coordinates. The TLSDO vector is composed from total landslide displacement TLSD and total landslide orientation, which indicates the orientation and displacement measured relative to the N direction.

A. Spatial deformation of strain gauges

Precise strain gauge placement on the measurement pole is an important factor in maintaining measurement accuracy for landslide displacement and orientation. Placement of the four strain gauges onto the measurement pole is shown in Figure 4. Strain gauges were placed 90 degrees apart and axially oriented along the pole. This setup facilitates a precise and sensitive measurement process for the smallest displacements of the land surface. A measurement pole contains multiple measurement nodes positioned two meters apart from each other onto the length of the pole. Multiple measurement points were positioned across the possible landslide area with the reference strain gauge facing the N cardinal direction. This placement was used to establish a polar reference system relatively to which we could further measure landslide displacement and orientation. Figure 4(a) presents the placement of strain gauges that form a measurement node. A possible landslide is represented here as a displacement vector D orientated with α degrees relative to North reference. The influence of landslide displacement over our measurement system is presented in Figure 4(b). One can observe that a landslide displacement with α degree orientated relative to N direction deforms the measurement pole and causes changes of each strain gauge impedance by giant magnetoimpedance effect [11],[12]. This produces unbalance of the measurement bridge leading to amplitude variations of the two potentials, U_a and U_b (Figure 3).

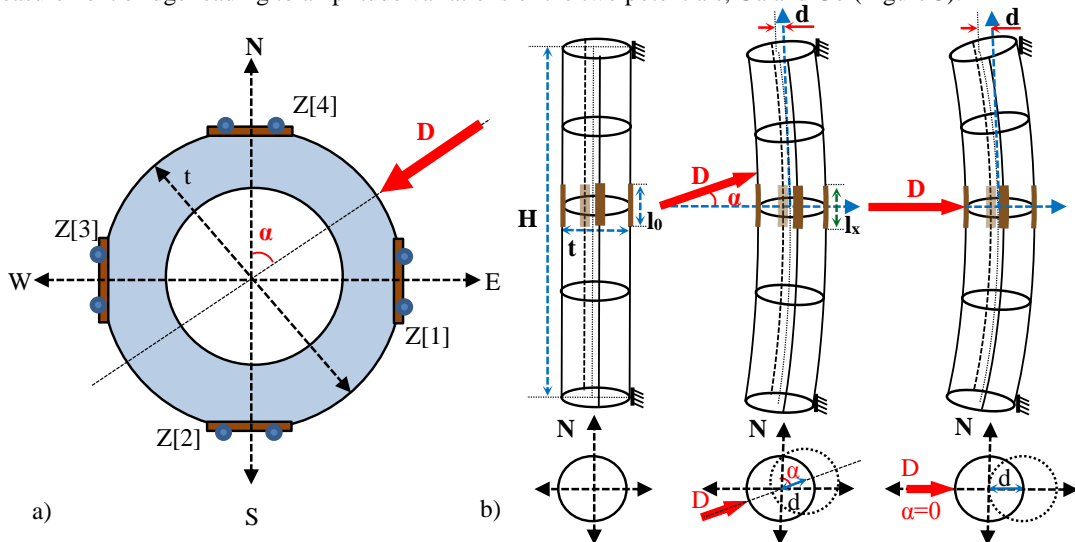


Figure 4. a) Placement of the strain gauges on the measurement pole, b) various stages of deformation caused by landslide displacements

The spatial deformation model of a strain gauge is computed starting from the basic characterization of a deformation oriented perpendicular on it. Gauge factor (GF) is given by (1).

$$GF = \frac{\Delta Z}{Z} \frac{1}{\varepsilon} = \frac{Z - Z_0}{Z} \frac{1}{\varepsilon}; GF \approx 1700 \quad (1)$$

Where ΔZ is the impedance change caused by strain, Z_0 is the impedance of the undeformed gauge, here called "nominal strain gauge impedance" and ε is the strain. Equation (2) I used in order to evaluate ε , where Δl is the total elongation and l_0 is the initial length.

$$\varepsilon = \frac{\Delta l}{l_0} = \frac{td}{\left(\frac{H}{2}\right)^2 + d^2} \quad (2)$$

In the above relation, according to Figure 4, H is the distance between two measurement nodes, d is the pole displacement, t is the pole diameter, l_x is the new length of the gauge, and D is the radius of the arc produced by bending the pole during the landslide. Because of their placement on the measurement pole, the four strain gauges deform differently in response the displacement caused by landslide. In order to calculate the deformation of each SG, of amplitude D and orientation α relative to the N direction we expressed the distance t_p between the application of the displacement and the spatial placement of a strain gauge (3).

$$\varepsilon = \frac{td}{\left(\frac{H}{2}\right)^2 + d^2} \cos(\alpha), \text{ where } \varepsilon_{\max} = \frac{td}{\left(\frac{H}{2}\right)^2 + d^2} \quad (3)$$

Using this model we could compute the spatial deformations of each strain gauge (4).

$$\begin{aligned} \varepsilon_N &= \varepsilon_{\max} \cos(\alpha + 0); & \varepsilon_E &= \varepsilon_{\max} \cos(\alpha + 90) \\ \varepsilon_S &= \varepsilon_{\max} \cos(\alpha + 180); & \varepsilon_W &= \varepsilon_{\max} \cos(\alpha + 270) \end{aligned} \quad (4)$$

The spatial deformation is computed using a maximum possible deformation ε_{\max} applied at α degree for each SG. Strain gauge placement on the measurement pole is reflected in the computation of deformation by means of an initial angle that is used to model the overall deformation effect (4). Depending on the initial placement of each strain gauge the deformation computation model receives an initial angle. Initial placement is described relative to N direction. Therefore the SG orientated in North direction receives an initial angle of 0 degrees, describing the compression process. The strain gauge orientated South, receives an initial angle of 180 degrees that reflects the tensioning of the string gauge. Following this model the East and West orientated strain gauges each receive an initial angle of 90 respectively 270 degrees. Final spatial deformation model uses the maximum deformation which is modulated by an initial orientation angle and the angle of the landslide displacement (4). Considering GF of our SG measurement sensors defined in (1) and taking into consideration the spatial deformation of the measurement system we have computed the variation in impedance that are used in the measurement setup for landslide displacement (5).

$$\begin{aligned} Z_N(\alpha) &= Z_0(GF_{N4} * \varepsilon_{\max} \cos(\alpha + 0) - 1); & Z_E(\alpha) &= Z_0(GF_{E1} * \varepsilon_{\max} \cos(\alpha + 90) - 1) \\ Z_S(\alpha) &= Z_0(GF_{S2} * \varepsilon_{\max} \cos(\alpha + 180) - 1); & Z_W(\alpha) &= Z_0(GF_{W3} * \varepsilon_{\max} \cos(\alpha + 270) - 1) \end{aligned} \quad (5)$$

B. Computation of landslide displacement and orientation

Impedance variation of SG was identified as a dependency function of variables α and ε_{\max} . Landslide displacement orientation α , and landslide displacement D measured relative to the North cardinal direction were computed using the two measured potentials U_a and U_b . Potentials U_a , U_b were calculated using equations (6).

$$U_a = E \frac{Z_W}{Z_E + Z_W}; \quad U_b = E \frac{Z_N}{Z_S + Z_N} \quad (6)$$

Using (5) and (6) we have expressed the potentials that describe the two branches of the measurement bridge (7).

$$\begin{aligned} U_a &= E \frac{Z_0(GF_W \varepsilon_{\max} \cos(\alpha + 270) - 1)}{Z_0(GF_E \varepsilon_{\max} \cos(\alpha + 90) - 1) + Z_0(GF_W \varepsilon_{\max} \cos(\alpha + 270) - 1)} \\ U_b &= E \frac{Z_0(GF_{N4} \varepsilon_{\max} \cos(\alpha + 0) - 1)}{Z_0(GF_S \varepsilon_{\max} \cos(\alpha + 180) - 1) + Z_0(GF_N \varepsilon_{\max} \cos(\alpha + 0) - 1)} \end{aligned} \quad (7)$$

In (7) the only unknown is α that specifies the orientation of the landslide, which is determined using the measured values of U_a , U_b , the maximum measured deformation ε_{\max} , the strain gauge factor GF, initial impedance value Z_0 , amplitude of the excitation signal E and initial strain gauge placement. The parameters ε_{\max} , Z_0 and GF have similar values for all SG that are taken into consideration when we determine landslide orientation components (8).

$$\sin(\alpha) = \frac{U_a GF \varepsilon_{\max} - E + 2U_a}{EGF \varepsilon_{\max}}; \quad \cos(\alpha) = -\frac{U_b GF \varepsilon_{\max} - E + 2U_b}{EGF \varepsilon_{\max}} \quad (8)$$

Final landslide orientation (FLSO_N) relative to North direction is expressed as a dependency of measured potentials U_a and U_b (9).

$$FLSO_N = \alpha(U_a, U_b) = \tan^{-1} \left(-\frac{U_a GF \varepsilon_{\max} - E + 2U_a}{U_b GF \varepsilon_{\max} - E + 2U_b} \right) \quad (9)$$

Landslide displacement (LSD) is determinate for cardinal directions taking into consideration the deformation model in which we substitute the FLSO_N already calculated. From (2), (3) and (4) we determine landslide displacement for cardinal directions (10), as the solutions to the resulted complex equations system.

$$\begin{aligned} LSD_N &= \frac{t \pm \sqrt{t^2 + 4 \left(\frac{U_b GF \varepsilon_{\max} - E + 2U_b}{EGF} \right)^2}}{\frac{2U_b GF \varepsilon_{\max} - 2E + 4U_b}{EGF}}; & LSD_E &= \frac{t \pm \sqrt{t^2 - 4 \left(\frac{U_a GF \varepsilon_{\max} - E + 2U_a}{EGF} \right)^2}}{\frac{2U_a GF \varepsilon_{\max} - 2E + 4U_a}{EGF}} \\ LSD_S &= \frac{t \pm \sqrt{t^2 + 4 \left(\frac{U_b GF \varepsilon_{\max} - E + 2U_b}{E + GF} \right)^2}}{\frac{2U_b GF \varepsilon_{\max} - 2E + 4U_b}{EGF}}; & LSD_W &= \frac{t \pm \sqrt{t^2 - 4 \left(\frac{U_a GF \varepsilon_{\max} - E + 2U_a}{EGF} \right)^2}}{\frac{2U_a GF \varepsilon_{\max} - 2E + 4U_a}{EGF}} \end{aligned} \quad (10)$$

Determined solutions (10) denote displacements consistent to four cardinal directions. One could observe that the displacements associated to North and South directions were similar in amplitude and opposite in sign. This indicates that the deformation measured relative to the South direction has an opposite sign reported to North direction. This observation also applies for East and West cardinal directions. If we are to represent the landslide displacement and orientation relative to North cardinal direction in polar coordinates a resulting total displacement is calculated as a vector sum of displacements corresponding to the North and East orientations. Landslide displacement and orientation that describe the deformation of the measurement pole for North ($LSDO_N$) and East ($LSDO_E$) directions are expressed in polar coordinates in equations (11).

$$LSDO_N = \left(\frac{t + \sqrt{t^2 + 4 \left(\frac{U_b GF \epsilon_{max} - E + 2U_b}{EGF} \right)^2}}{2U_b GF \epsilon_{max} - 2E + 4U_b}, \cos^{-1} \left(- \frac{U_b GF \epsilon_{max} - E + 2U_b}{EGF \epsilon_{max}} \right) \right)$$

$$LSDO_E = \left(\frac{t + \sqrt{t^2 - 4 \left(\frac{U_a GF \epsilon_{max} - E + 2U_a}{EGF} \right)^2}}{2U_a GF \epsilon_{max} - 2E + 4U_a}, \sin^{-1} \left(\frac{U_a GF \epsilon_{max} - E + 2U_a}{EGF \epsilon_{max}} \right) \right)$$
(11)

Final landslide orientation and displacement ($FLSDO_N$) is computed as the sum of the two components and is represented in polar coordinates relative to the North direction (12).

$$FLSDO_N(U_a, U_b) = \left(\frac{\sqrt{|d_N(U_a, U_b)|^2 + |d_E(U_a, U_b)|^2}}{2}, \tan^{-1} \left(- \frac{U_a GF \epsilon_{max} - E + 2U_a}{U_b GF \epsilon_{max} - E + 2U_b} \right) \right)$$
(12)

The presented mathematical model is integrated inside the software that runs continuously on the microcontroller managing a measurement node and it is used to compute landslide displacement and orientation. Nodes compute landslide displacement and orientation using potentials acquired from measurement bridges. Data from measurement nodes provide a complete perspective regarding the landslide displacement influencing measurement points. This process gives us precise data about earth layers that are presenting relative movements relative to North direction. Large landslide areas could be accurately surveyed using a grid of measurement points that convey measurement data to a central server capable of creating distress alerts in case of a pending landslide risk.

IV. Experimental results and discussion

We have investigated the performance of our landslide measurement system in terms of the computed landslide displacement and orientation with respect to measured references for displacement and orientation. In our experimental setup we have submitted a measurement pole having a length of 2000mm and a diameter of 25 mm on which were bonded for SG connected in a bridge configuration, to a displacement of 45mm with a variable orientation measured relative to North direction. Table 1 presents computation results returned by our measurement system for displacement d and orientation α , based on the presented mathematical model.

Table 1. Experimental results regarding landslide displacement and orientation

Reference Orientation	N	NE		E	SE		S	SW		W	NW		N
	0	30	60	90	120	150	180	210	240	270	300	330	360
α measured	1.2	28.5	61.3	88.7	119.2	148.9	180.7	209.2	241.1	268.9	298.5	328.6	360.3
d measured	44.8	44.4	45.3	45.7	46.1	45.2	44.6	45.1	44.8	44.3	45.7	45.3	45.1

In order to calculate these results, the model used the following values for the involved parameters: $t=25$ mm, $\epsilon_{max}=575 \times 10^{-9}$, $GF=1700$, $E_{pk-pk}=56$ mV. Measured potentials U_a , U_b were ranging from 15 mV to 40 mV. Displacement was applied to the measurement pole with an incremental orientation of 30 degrees from 0 to 360 degrees. For each referenced displacement an orientation, (ex: $\alpha=30^\circ$, $d=45$ mm) the system returns a calculated displacement and orientation (ex: $\alpha=28.5^\circ$, $d=44.4$ mm). Precision of the measurement process for landslide movements is affected by the following error sources: errors caused by the uniformity of the MAW used to create SG, imperfect electrical contact between MAW and solder pads, nonlinear variation of impedance. Absolute errors determined for landslide displacement and orientation are presented in Figure 4. One can observe that absolute error specific to displacement computation $\Delta\alpha_{max}$ has a maximum value of 2. Absolute error specific to orientation calculation $\Delta\alpha_{max}$ reaches a maximum value of 3.

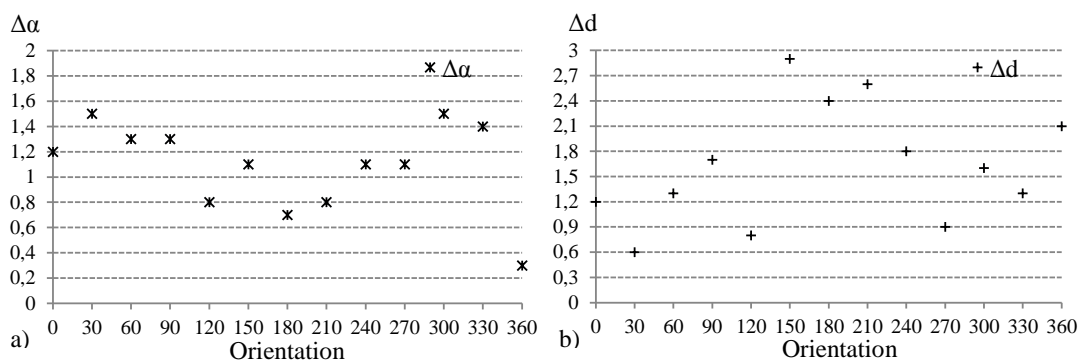


Figure 5. Absolute errors specific for displacement and orientation measurement procedure, a) orientation absolute error, b) displacement absolute error

V. Conclusions

A study regarding the possibility of using an MAW strain gauge to measure landslide displacement and orientation has been performed in this paper. We have tested our measurement point using an experimental setup in laboratory conditions and have found that the system is capable of measuring displacement in the range of 1-200 mm that could possibly have orientations measured with 0.1 degrees accuracy in range of 0-360 degrees. Thus, we have developed a precise measurement system for landslide displacement and orientation based on MAW strain gauges. The system measures the displacement and orientation of landslides based on the two measured potentials U_a and U_b and the presented computational model. Measurements are done at each measurement node by a microcontroller that sends the measured parameters to a central unit coordinator via RS485 communication protocol. We have used the RS485 communication protocol to transmit data packages between measurement nodes and unit coordinator because of its advantages in terms of communication distance and reliability. The presented system offers the advantages of a low cost precise and accurate measurement system for landslide displacements, low power consumption, continuous measurements and wireless data communication between the measurement grid and a central server.

Acknowledgment

The results presented in this paper have been financially supported by the Romanian Ministry of Education and Research through the project PN-II-PT-PCCA-2011-3.2-0975, contract no. 63/2012.

References

- [1] Malet, J.-P., Maquaire, O., Calais, E., The use of Global Positioning System techniques for the continuous monitoring of landslides, *Geomorphology*, Vol. 43, pp. 33–54, (2002).
- [2] Mora P., Baldi P., Casula G., Fabris M., Ghirotti M., Mazzini E., Global Positioning Systems and digital photogrammetry for the monitoring of mass movements, *Engineering Geology*, Vol. 68, pp. 103–121, (2003).
- [3] Xiaobing Zhou, Ni-Bin Chang, Shusun Li, Applications of SAR Interferometry in Earth and Environmental Science Research, *Sensors*, 9, pp.1876-1912; 2009.
- [4] Corsini, A., Borgatti, L., Coren, F., and Vellico, M., Use of multitemporal airborne lidar surveys to analyse post-failure behaviour of earthslides, *Canadian Journal of Remote Sensing*, 33(2), pp.116-120, 2007;
- [5] Janet E. Nichol, Ahmed Shaker, Man-Sing Wong, Application of high-resolution stereo satellite images to detailed landslide hazard assessment, *Geomorphology*, 76, pp. 68–75, 2006.
- [6] Gili, J.A., Corominas, J., Rius, J., Using Global Positioning System techniques in landslide monitoring, *Engineering Geology*, 55, pp.167–192, 2000.
- [7] K. Higuchi, K. Fujisawa, K. Asai, A. Pasuto, Application Of New Landslide Monitoring Technique Using Optical Fiber Sensor, Takisaka Landslide, Society for study of Optical Fiber Sensors, JAPAN.
- [8] Alberto Rosi, Nicola Bicocchi, Gabriella Castelli, Marco Mamei, Franco Zambonelli, Landslide Monitoring with Sensor Networks: Experiences and Lessons Learnt from a Real-World Deployment.
- [9] C. Fosalau, C. Damian, C. Zet, A high performance strain gage based on the stressimpedance effect in magnetic amorphous wires, *Sensors and Actuators A* 19, pp.105–110, 2013.
- [10] H. Chiriac and T.-A. Óvári, “Novel trends in the study of magnetically soft Co-based amorphous glass-coated wires”, *J. Magn. Magn. Mater.*, vol. 323, pp. 2929-2940, 2011.
- [11] M. Vázquez, H. Chiriac, A. Zhukov, L. Panina, and T. Uchiyama, “On the state-of-the-art in magnetic microwires and expected trends for scientific and technological studies”, *Phys. Stat. Sol. (a)*, Vol. 208, pp. 493-501, 2011.
- [12] S. Corodeanu, T.-A. Óvári, N. Lupu, “Magnetization process and GMI effect in as-cast nanocrystalline microwires”, *IEEE Trans. Magn.*, Vol. 46, pp. 380-382, 2010.